Journal of Controlled Release 205 (2015) 181–189

Contents lists available at ScienceDirect

Journal of Controlled Release

journal homepage: www.elsevier.com/locate/jconrel

Poly(amido amine)-based multilayered thin films on 2D and 3D supports for surface-mediated cell transfection

Sry D. Hujaya [a,1], Giulia Marchioli [b,c,1], Karin Roelofs [a], Aart A. van Apeldoorn [b], Lorenzo Moroni [c], Marcel Karperien [b], Jos M.J. Paulusse [a,*], Johan F.J. Engbersen [a,*]

[a] Department of Controlled Drug Delivery, University of Twente, P.O. Box 217, 7500 AE Enschede, The Netherlands
[b] Department of Developmental BioEngineering, University of Twente, P.O. Box 217, 7500 AE Enschede, The Netherlands
[c] Department of Tissue Regeneration, University of Twente, P.O. Box 217, 7500 AE Enschede, The Netherlands

ARTICLE INFO

Article history:
Received 30 November 2014
Received in revised form 20 January 2015
Accepted 27 January 2015
Available online 28 January 2015

Keywords:
Multilayered thin films
Layer-by-layer assembly
Biodegradable polymers
Cell transfection
Gene delivery

ABSTRACT

Two linear poly(amido amine)s, pCABOL and pCHIS, prepared by polyaddition of cystamine bisacrylamide (C) with 4-aminobutanol (ABOL) or histamine (HIS), were explored to form alternating multilayer thin films with DNA to obtain functionalized materials with transfection capacity in 2D and 3D. Therefore, COS-7 cells were cultured on top of multilayer films formed by layer-by-layer dipcoating of these polymers with GFP-encoded pDNA, and the effect of the number of layers and cell seeding density on the transfection efficiency was evaluated. Multilayer films with pCABOL were found to be superior to pCHIS in facilitating transfection, which was attributed to higher incorporation of pDNA and release of the transfection agent. High amounts of transfected cells were obtained on pCABOL films, correlating proportionally over a wide range with seeding density. Optimal transfection efficiency was obtained with pCABOL films composed of 10 bilayers. Further increase in the number of bilayers only marginally increased transfection efficiency.

Using the optimal multilayer and cell seeding conditions, pCABOL multilayers were fabricated on poly(ε-caprolactone) (PCL), heparinized PCL (PCL-HEP), and poly(lactic acid) (PLA) disks as examples of common biomedical supports. The multilayers were found to completely mask the properties of the original substrates, with significant improvement in cell adhesion, which is especially pronounced for PCL and PLA disks. With all these substrates, transfection efficiency was found to be in the range of 25–50% transfected cells. The pCABOL/pDNA multilayer films can also conveniently add transfection capability to 3D scaffolds. Significant improvement in cell adhesion was observed after multilayer coating of 3D-plotted fibers of PCL (with and without an additional covalent heparin layer), especially for the PCL scaffold without heparin layer and transfection was observed on both 3D PCL and PCL-HEP scaffolds. These results show that layer-by-layer dip-coating of pCABOL with functional DNA is an easy and inexpensive method to introduce transfection capability to biomaterials of any nature and shape, which can be beneficially used in various biomedical and tissue engineering applications.

1. Introduction

The layer-by-layer (LbL) fabrication technique has emerged as a versatile way not only to modify or improve surface properties, but also to add functionalities to the surface of various biomedical materials [1–4]. For example, a substantial development in tissue engineering relies on scaffolds for mechanical cell support and many medical operations involve mechanical support devices such as stents, prostheses, and other implants that have specific shapes and sizes. Often these devices are made of specific materials chosen for their mechanical strength and biodegradability, but do not really provide optimal performance in their interactions with cells [5]. LbL assembly offers an excellent option to add functionality to biomedical materials by coating various substrates with thin multilayers of functional macromolecules simply by dipping the substrates alternately into two aqueous solutions containing the desired macromolecules. The resulting surface can promote or reduce cell adhesion [6–8], deliver small drugs [9–11] or therapeutic proteins [12–15], induce differentiation [16–19] and cell transfection [20–22]. Moreover, the concentration and variety of material incorporation and release can be adjusted simply by adding or reducing the deposition cycles.

A promising application for LbL assembly that has recently received increasing attention is surface-mediated cell transfection [23]. As early as 1993, Lvov et al. reported the preparation of a multilayer using DNA as a building block [24]. Since then, several research groups, notably the groups of Lynn and Hammond, have studied the potential of LbL-based multilayers to provide localized delivery of transcriptionally

* Corresponding authors.
E-mail addresses: J.M.J.Paulusse@utwente.nl (J.M.J. Paulusse), J.F.J.Engbersen@utwente.nl (J.F.J. Engbersen).
[1] These authors contributed equally.

http://dx.doi.org/10.1016/j.jconrel.2015.01.034
0168-3659/

active DNA [22,23,25–28]. The DNA may be deposited between the layers [20,25], or pre-complexed with polymers into polyplexes [29,30]. Notably, surface-mediated cell transfection has been attempted on intravascular stents [26,27], flexible stainless steel [20], poly(D-lactic acid) film [31], and micro-needles [28] aimed for vaccination application [32,33].

Multilayer coatings for surface-mediated transfection purposes on 3D scaffolds for tissue engineering have not been extensively reported. Attempts to introduce transfection capability to 3D scaffolds are mostly carried out before [34,35] or after [36–38] seeding into the scaffolds, by loading the plasmid or polyplex into the matrix of the scaffolds [39,40] or adsorbing on the surface [41–43]. Mineral coatings have also been reported, most notably CaP [44], which was incubated with lipoplexes to induce transfection upon cell seeding [45]. Compared to these techniques, LbL dipping technique offers the possibility to design more intricate multilayer design for prolonged or scheduled release [46] of multiple components. Moreover, the aqueous conditions for formation of the LbL films enable to preserve native structures of functional macromolecules. As a recent example, Holmes et al. reported coating of 3D scaffolds with multilayers of glycol-chitosan and hyaluronic acid. The multilayer-coated scaffolds were found to enhance tissue growth relative to non-coated scaffolds, and additional transfection capability could be observed by depositing a layer of DNA-containing lipoplexes [47]. Hammond and co-workers have reported the multilayer assembly on poly(lactic-co-glycolic acid) molded into microneedle arrays for transcutaneous delivery of plasmid DNA [28]. The multilayer-coated microneedles successfully induced transfection on mice in vivo.

To enable multilayer formation, a pair of macromolecules is needed that interact with each other. For negatively-charged DNA, a positively-charged biocompatible polymer may serve as a good counterpart. Poly(β-amino ester) (PBAE) introduced by the group of Lynn, is one of the most extensively studied polymer for this purpose [22,25–28]. In this paper we report on the preparation and properties of multilayers of DNA with bioreducible linear poly(amido amine)s (PAA). Poly(amido amine)s are a class of peptidomimetic polymers synthesized via Michael-type addition polymerization of amines and bisacrylamides. Through the presence of amide bonds, PAAs are inherently biodegradable through hydrolysis. Moreover, through the availability of various building blocks, these polymers can also be designed to incorporate various moieties for added functionality such as charge-shift, bioreducibility, 'stealth' properties and targeting moieties [48–50].

Here, we report the fabrication, characterization and cell transfection properties of multilayered thin films of DNA with pCABOL and pCHIS, respectively. These linear, bioreducible PAAs were selected because these polymers have previously shown to be two of the best performing PAAs in polyplex systems for cell transfection [51]. Cell transfection efficiency of the multilayers was optimized using flow cytometry as an analytical tool to determine transfection efficiency as a function of the PAA type, cell seeding density, and layer number. Finally, with the optimized conditions, surface-mediated cell transfection was accomplished on poly(ε-caprolactone) (PCL), heparinized PCL (PCL-HEP), and poly(lactic acid) (PLA) substrates, both in 2D (disk shape) and 3D (fiber deposited PCL and PCL-HEP).

2. Materials and methods

2.1. Chemicals, syntheses and characterization

N,*N*′-Cystamine bisacrylamide (CBA, Polysciences), 4-amino-1-butanol (ABOL, Sigma-Aldrich, Zwijndrecht, The Netherlands), *N*-Boc-1,4-diaminobutane (NBDAB, Sigma-Aldrich, Zwijndrecht, The Netherlands), histamine dihydrochloride (HIS·2HCl, Sigma-Aldrich, Zwijndrecht, The Netherlands), calcium chloride ($CaCl_2$, Sigma-Aldrich, Zwijndrecht, The Netherlands), triethylamine (TEA, Sigma-Aldrich, Zwijndrecht, The Netherlands), *tert*-butylamine (*t*BA, Sigma-Aldrich, Zwijndrecht, The Netherlands), sodium dihydrogen phosphate monohydrate ($NaH_2PO_4 \cdot H_2O$, Merck, Darmstadt, Germany), disodium hydrogen phosphate dihydrate ($Na_2HPO_4 \cdot 2H_2O$, Merck, Darmstadt, Germany), sodium chloride (NaCl, Sigma-Aldrich, Zwijndrecht, The Netherlands), dithiothreitol (DTT, Sigma-Aldrich, Zwijndrecht, The Netherlands), 4-(2-Hydroxyethyl)piperazine-1-ethanesulfonic acid (HEPES, Sigma-Aldrich, Zwijndrecht, The Netherlands) and glucose (Sigma-Aldrich, Zwijndrecht, The Netherlands) were purchased in the highest purity available and used as received. Solvents were of reagent grade and used without further purification unless otherwise noted. Milli-Q water was obtained from a Synergy® water purification system (Millipore). PBS buffer was prepared by dissolving 1.54 g of $Na_2HPO_4 \cdot 2H_2O$, 0.3 g of $NaH_2PO_4 \cdot H_2O$, and 8.2 g of NaCl into 1 L of Milli-Q water and adjusting the pH to 7.4. HEPES buffered glucose (HBG) was prepared by dissolving 4.79 g of HEPES, and 50 g of glucose into 1 L of Milli-Q water and adjusting the pH to 7.4.

2.2. Polymer synthesis

The PAA polymers pCABOL and pCHIS were synthesized by polyaddition of cystamine bisacrylamide (C) with 4-aminobutanol (ABOL) or histamine (HIS) according to modified literature procedures [51]. Therefore, in a brown polymerization flask containing 2 mL methanol/water 3/1 and 200 mM $CaCl_2$ as catalyst, *N*,*N*′-cystamine bisacrylamide (1.04 g; 4.0 mmol) was mixed with an equimolar amount of 4-amino-1-butanol (0.37 g) or histamine dihydrochloride (0.74 g), respectively [52]. Polymerization was carried out under N_2 atmosphere for two days at 70 °C during which a gradual viscosity increase was observed. The polymerization was terminated by adding excess *tert*-butylamine into the mixture and stirring at 70 °C for two or three more days. After bringing the flask to room temperature, the solution was diluted and acidified to pH ~5 by addition of 4 M HCl and purified by ultrafiltration using a 1000 Da MWCO membrane. The purified polymer solution was then freeze-dried leaving white transparent solid as the final product in its HCl-salt form at ~50% recovery. ^{1}H NMR spectroscopy confirmed complete termination and allowed determination of the number-average MW based on the *tert*-butylamine end-group. ^{1}H NMR spectra were recorded on an AVANCE III-400 MHz NMR (Bruker, Wormer, The Netherlands) spectrometer. Gel permeation chromatograms were recorded on a Polymer Labs GPC 220 in 0.1 M NaOAc buffer pH 4 with 25% methanol as eluent and 0.7 mL/min flow rate against poly(ethylene glycol) (PEG) standards. pCABOL ^{1}H NMR (D_2O) δ (ppm) = 1.35 (s, 9H, $(CH_3)_3R$); 1.60 (m, 2H, CH_2CH_2NR); 1.77 (m, 2H, CH_2CH_2OH); 2.74 (t, 4H, $CH_2CONHRNHCOCH_2$); 2.85 (t, 4H, CH_2SSCH_2); 3.22 (t, 2H, $HO(CH_2)_3CH2NR$); 3.44 (t, 4H, $NCOCH_2CH_2NRCH_2$); 3.53 (t, 4H, $CH_2CH_2SSCH_2CH_2$); and 3.62 (t, 2H, CH_2OH). ^{1}H NMR end group analysis M_w = 9 kg/mol. GPC M_w = 3.8 kg/mol (M_w/M_n = 1.18). pCHIS ^{1}H NMR (D_2O) δ (ppm) = 1.39 (s, 9H, $(CH_3)_3R$); 2.78–2.95 (m, 8H, $CH_2CONHRNHCOCH_2$ & CH_2SSCH_2); 3.23 (t, 2H, CCH_2); 3.48–3.80 (m, 10H, $(CH_2)_3$ N & $CH_2CH_2SSCH_2CH_2$); 7.45 (s, 1H, NC = C*H*); and 8.71 (s, 1H, N = C*H*). ^{1}H NMR end group analysis M_w = 5.5 kg/mol. GPC M_w = 4.6 kg/mol (M_w/M_n = 1.26).

2.3. Substrate preparation

Poly-D-lysine-coated 96-well plates (PDL–TCPS) for multilayer build-up for cell culture and transfection experiments were purchased from Greiner (Alphen aan den Rijn, The Netherlands).

Poly(lactic acid) (PLA) sheets with a thickness of 120 μm were kindly provided by Sidaplax (Ghent, Belgium) and cut in 6 mm diameter disks with a biopsy puncher (Miltex, Rietheim — Weilheim, Germany).

Poly(ε-caprolactone) (PCL) M_w 45,000 was purchased from Sigma, (Zwijndrecht, The Netherlands). 2D disks were fabricated by placing the PCL grains in between two hydrophobic silica wafers and heating the PCL grains in a press at 100 °C. Pressure was applied to the molten polymer. After cooling, the polymer sheet was removed from the press and

disks of 6 mm in diameter were punched out from the polymer sheet with a biopsy puncher.

Poly(ε-caprolactone) 3D plotted scaffolds were fabricated using additive manufacturing (sysENG, Germany). Scaffolds presented a toroidal shape and were 8 mm in the outer diameter and 4 mm in the inner diameter. The scaffold thickness was 1 mm. PCL with a molecular weight of 45,000 was heated to 100 °C before being extruded from a needle of 200 μm in diameter. Plotting speed and pressure were set to 175 mm/min and 5 bars, respectively. Scaffolds were plotted in a 0–90 fiber deposition configuration, with a fiber spacing of 600 μm and a layer thickness of 150 μm.

Covalent immobilization of heparin (HEP) on the PCL sheets and 3D plotted PCL was performed by dissolving 1% (w/v) heparin (Sigma, Zwijndrecht, The Netherlands) in 0.05 M 2-(N-morpholino) ethanesulfonic acid (MES) buffer (Sigma, Zwijndrecht, The Netherlands) at pH 5.5. 1-Ethyl-3-(3-dimethylaminopropyl)carbodiimide (EDC) and N-Hydroxysuccinimide (NHS) (Sigma, Zwijndrecht, The Netherlands) were added at a concentration of 0.5 M to the heparin solution, vigorously stirred and added to the PCL disks. After 15 h reaction at room temperature, the disks were extensively washed with water [53,54].

2.4. Multilayer construction

Multilayers for cell culture were fabricated directly in the wells of poly-D-lysine-coated 96-well plates (PDL–TCPS, Greiner) by alternatingly dispensing 70 μL of plasmid DNA (1 mg/mL in sterile water) and poly(amido amine) (PAA) (2 mg/mL in PBS pH 7.4) with washing solutions in between, which consisted of the solvents of the respective deposition solutions (2× 150 μL). The layer-by-layer (LbL) deposition was performed under sterile conditions. The DNA used to induce cell transfection was plasmid DNA encoding for green fluorescent protein (GFP) as a reporter gene and its expression was controlled by a cytomegalovirus promotor (PlasmidFactory, Bielefeld, Germany). This construct will be referred as pCMV-GFP and it was used at a 1 mg/mL concentration in sterile water. The resulting ensemble is denoted by $(\text{pCMV-GFP\#PAA})_{\mathbf{n}}$, where PAA represents the identity of the poly(amido amine), and **n** represents the number of bilayer. Typically, the ensemble consists of 10 bilayers with the plasmid DNA as the first layer. Deposition started with pCMV-GFP (30 min for the first layer, 10 min next) to a total of 10 bilayers, ending with the PAA layer. No intermediate drying steps were applied. At the end of the fabrication process, the plates were briefly left inside the laminar flow hood to allow the films to dry. Coated plates were kept at 4 °C and used as soon as possible (typically overnight).

LbL assembly on the 2D disks and 3D plotted constructs was carried out by alternate dipping of the PCL and PCL-HEP constructs in sufficient volume of 2 mg/mL pCABOL and 1 mg/mL pCMV-GFP solutions. Unlike for multilayer fabrication on PDL–TCPS, deposition on 2D and 3D constructs started with pCABOL layer as a precursor layer with 30 min deposition duration. Next deposition steps were 10 minute long followed by two washing steps for 1 min each. Typical multilayer on 2D and 3D constructs is denoted by $\text{pCABOL-(pCMV-GFP\#pCABOL)}_{\mathbf{10}}$ to indicate the presence of a pCABOL layer as a precursor layer that is excluded from the bilayer count. Multilayer-coated 2D disks were glued on the bottom of regular polystyrene 96-well plates using silicone glue. For 3D scaffolds, three scaffolds were simultaneously coated in the same 48-well as the container. The constructs were left to dry in the laminar flow hood or with nitrogen stream at the end of the assembly and kept at 4 °C until use.

Scanning electron microscopy (SEM) of the 3D plotted PCL and heparin-coated PCL scaffolds, with or without multilayers were carried out following gold sputtering of samples (Cressington sputter coater 108 auto) on a Philips — XL 30 ESEM-FEG. SEM images were taken with an accelerating voltage of 5 kV.

2.5. Cell culture, transfection and metabolic activity

COS-7 cells (European Collection of Animal Cell Cultures (ECACC) Catalogue No. 87021302) were grown in DMEM containing 4.5 g/L glucose and GlutaMAX™ (Invitrogen, Breda, The Netherlands) supplemented with 1% (v/v) Pen/Strep (Lonza, Breda, The Netherlands) and 10% (v/v) fetal bovine serum (Lonza, Breda, The Netherlands). Cells were cultured at 37 °C, in a 5% CO_2 incubator and trypsinized at about 80% confluency. Unless otherwise specified, cells were seeded in a 96-well plate at a density of 7360, 24,000 or 44,800 cells/well. On the 3D plotted constructs, cells were seeded at a density of 320,000 cells/construct in four small droplets of 80 μL each.

Cell imaging was performed using an EVOS digital inverted microscope (EMS, Wageningen, The Netherlands) equipped with a 4× objective and an EVOS light cube (EMS, Wageningen, The Netherlands) for GFP imaging.

Presto blue assay for the measurement of cell metabolic activity was purchased from Invitrogen (Breda, The Netherlands) and used according to the manufacturer's instructions. Fluorescence intensity was measured at 535–560/590–615 ex/em using an Infinite M200 PRO plate reader (Tecan, Giessen, The Netherlands). As positive controls, cells were also seeded on uncoated TC-treated polystyrene well plates (TCPS). All fluorescence intensities were corrected by subtracting the values with those of their respective no-cell control wells. Metabolic activity was calculated as the percentage of fluorescence intensity of the samples relative to cells cultured on TCPS (100% metabolic activity). Experiments were done in triplicates.

2.6. Determination of transfection efficiency by flow cytometry

After 48 h culturing, COS-7 cells on multilayer-coated PDL–TCPS and on the polymer disks were trypsinized (100 μL of 0.25% trypsin solution, Invitrogen, Breda, The Netherlands). Cell suspensions were then centrifuged (5 min, 300 *g*, 1200 rpm) and the pellets were resuspended into 100 μL of medium. Cells were kept on ice until measurement by the FACSCalibur (Becton-Dickinson, Breda, The Netherlands). Excitation of expressed GFP was performed at 488 nm and emission was detected via a 530 nm band-pass filter. At least 4000 and 10,000 events were measured for samples with lower, intermediate and higher seeding density, respectively. Data analysis was performed using the FACS Cellquest Software. The gate setting was equal for all samples within the same experiment. Dot plot was applied to separate live cell population from dead cells and film residues. From the histogram obtained, marker was drawn to identify cells as live GFP-positive cells or GFP-negative cells.

2.7. PicoGreen assay and agarose gel electrophoresis

PicoGreen assay was performed to estimate the amount of DNA in the multilayers. Multilayered samples were prepared as described previously. At the end of the multilayer formation, pCMV-GFP and PAA deposition solutions were collected and diluted 500 times in sterile water. For calibration curve, clean unused pCMV-GFP solution of known concentration was first diluted 500 times in sterile water and then serially diluted. Finally, 10 μL of diluted solutions was transferred into black 96-well plate containing 90 μL of 1× PicoGreen solution in TE buffer, incubated for 5 min at RT in the dark and read for fluorescence intensity (485/520 ex/em) using the Infinite M200 PRO plate reader (Tecan, Giessen, The Netherlands). Direct method for pCMV-GFP concentration determination was carried out similarly, but each sample solution was retrieved from multilayer-coated well which had been incubated for 1 h in 200 μL of 4 mM DTT in PBS at pH 7.4 in the incubator.

For agarose gel electrophoresis, 200 μL of complete cell culture medium was added directly on top of multilayer-coated culture wells (prepared as described in Section 2) and incubated for 1 h in the incubator. Following the incubation, 21 μL of incubation medium was collected from each samples, mixed with 4 μL of loading buffer and loaded into a

1.5 wt% agarose gel (Bio-Rad) containing 1 × SYBR Safe (Invitrogen). Electrophoresis was run for 90 min at 90 V in TAE running buffer (40 mM tris(hydroxymethyl)aminomethane, 20 mM acetic acid, 1 mM EDTA, pH 8.2). Pictures were taken on a FluorChem M (ProteinSimple, Westburg, Leusden, The Netherlands) under UV illumination.

3. Results and discussion

The PAA polymers pCABOL and pCHIS were obtained in *ca.* 50% yield by polyaddition of cystamine bisacrylamide (C) with 4-aminobutanol (ABOL) or histamine (HIS), respectively [51]. Multilayered thin films of these cationic polymers with anionic plasmid DNA can be easily prepared by alternating exposure of substrates to aqueous solutions of these components. The detailed physical characterization of these thin films is described elsewhere [55]. In this study, the transfection capabilities of the multilayered systems were examined in relation to cell seeding density, type of PAA, and number of bilayers. Subsequently, the optimized conditions were used to build multilayers on several common biomedical materials, both in 2D and 3D, to endow cell transfection capabilities to these materials.

3.1. Effects of type of PAA and seeding density

To investigate whether cell seeding density influences cell transfection efficiency, COS-7 cells were seeded at three seeding densities, i.e. 7360 cells/well (23,000 cells/cm^2), 24,000 cells/well (70,000 cells/cm^2), and 44,800 cells/well (140,000 cells/cm^2). Transfection efficiency increased slightly going from 1 day to 2 days of culture along with increasing cell number, but no further significant increase was observed upon longer culture duration (data not shown). Thus, 2 days was found to be the optimal culture duration to determine transfection efficiency. Overlaid brightfield and GFP images of COS-7 cells cultured in three different seeding densities on $(pCMV\text{-}GFP\#pCABOL)_{\mathbf{10}}$ and $(pCMV\text{-}GFP\#pCHIS)_{\mathbf{10}}$ multilayers after 2 days of culture are shown in Fig. 1A. Excellent cell attachment was observed for both multilayers. After 2 days of culture, cells at the lowest seeding density have just reached confluency. Cells at the medium seeding density were notably more crowded, while cells at the highest seeding density were overconfluent with significantly more detached dead cells. The similar confluency on both multilayers indicates that the differences in the PAAs have no influence on cell proliferation rate. Fig. 1A also indicates qualitatively that the transfection efficiencies achieved by the two different multilayers depend on the seeding density of the cells on top of the multilayered films. For $(pCMV\text{-}GFP\#pCABOL)_{\mathbf{10}}$, an optimum in transfection efficiency was observed at the intermediate seeding density while for $(pCMV\text{-}GFP\#pCHIS)_{\mathbf{10}}$, the highest transfection efficiency was seen at the lowest seeding density.

To get a quantitative estimation of the transfection efficiency on all studied samples, flow cytometry was employed to count GFP-positive cells from the rest of the cell population. Fig. 1B shows the percentage

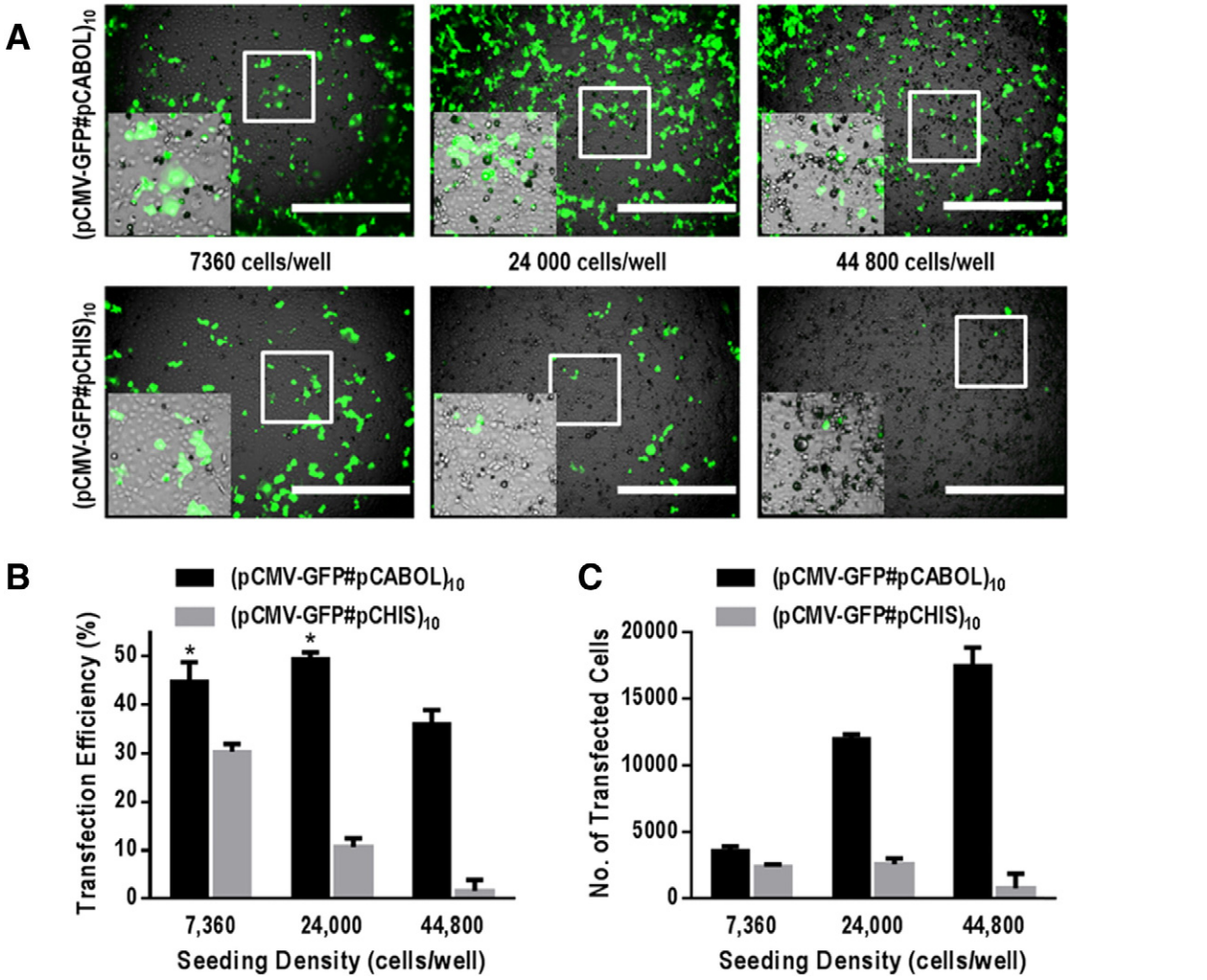

Fig. 1. (A) Overlaid brightfield and GFP images of COS-7 cells 48 h after being cultured on $(pCMV\text{-}GFP\#pCABOL)_{10}$ (top) and $(pCMV\text{-}GFP\#pCHIS)_{10}$ (bottom) at 7360 (left), 24,000 (middle), and 44,800 (right) cells/well seeding densities (scale bars = 1000 μm). Insets show the higher magnification to reveal the general cell morphology and confluency. (B) Transfection efficiency in percentage of total live cell population, and (C) absolute number of transfected cells irrespective to the total cell population.

of transfected cells in the total cell population in each sample. This graph agrees with the qualitative observation in Fig. 1A; at all different seeding densities used the pCABOL-multilayer provides higher transfection efficiency than the pCHIS-multilayer. Furthermore, the pCABOL-multilayer provides the highest transfection efficiency at intermediate seeding density (i.e. 24,000 cells/well), while the pCHIS-multilayer gives the highest transfection efficiency at the lowest seeding density (i.e. 7360 cells/well).

Fig. 1C shows the transfection efficiency in terms of absolute number of transfected cells produced on the multilayers at the three cell seeding densities. It is clear from this figure that the highest yield of transfected cells can be obtained when pCABOL-multilayers at the highest seeding density are used.

In relation to cell growth phase, optimal transfection efficiency is normally reached when the cells are in the log phase [56]. Therefore, the lowest seeding density which leads to ~95% confluency after 2 days of culture can be expected to provide the highest transfection efficiency, as is observed for the pCHIS system. Higher seeding density may lead to stationary or even death phase, where proliferation and subsequently production of GFP protein are no longer optimal.

Unlike the pCHIS system, pCABOL multilayers maintain optimal transfection efficiency up to the intermediate seeding density, before slightly reducing at the highest seeding density (Fig. 1B). The ability of pCABOL system to provide both higher transfection efficiency than pCHIS, and to maintain it up to the intermediate seeding density may be related to previous findings that pCABOL provides higher transfection efficiency than pCHIS when used as polyplex at the same polymer/DNA ratio [51]. Thus, pCABOL acts as a better transfection agent for DNA than pCHIS under the same conditions.

In a layer-by-layer multilayered thin film system, the ratio of polymer/DNA in a multilayer is largely determined by specific interactions between a given polymer–DNA pair. UV absorbance measurements at 260 nm on 10-bilayered films of both pCABOL and pCHIS indicated deposition of approximately similar amounts of DNA [55]. The pCHIS multilayer, however, contains significantly more polymer than the pCABOL multilayer, as was evident from the significantly higher thickness based on AFM. Thus, at the same number of bilayers, the pCHIS system contains a higher polymer/DNA ratio compared to the pCABOL system. This difference may further influence DNA packing and transfection capability of the multilayers. In order to gain more insight into the amount of incorporated pCMV-GFP in the two multilayered systems and to qualitatively observe differences in the release of polyplexes into cell culture medium, PicoGreen assay and agarose gel electrophoresis were employed, respectively.

The PicoGreen assay was utilized to estimate the amount of incorporated pCMV-GFP in the multilayers by comparing the decrease in pCMV-GFP concentration in the deposition solution before and after multilayer formation (Fig. 2A). From the assay, it was estimated that $(pCMV\text{-}GFP\#pCABOL)_{10}$ and $(pCMV\text{-}GFP\#pCHIS)_{10}$ multilayers coated on the surface of a 96-well plate contained 2.37 ± 0.13 and 1.96 ± 0.06 μg of pCMV-GFP, respectively. This leads to ~650, and ~540 ng/cm^2/layer, respectively, which falls within the broad range of reported values of DNA-containing multilayers [20,26,46,57]. It needs to be noted that this indirect method is based on the assumption that there is no change in the solution volume before and after the 10-bilayer deposition, and that there is no significant loss of pCMV-GFP during the washing steps. Nevertheless, both UV measurements at 260 nm and PicoGreen assay point to a slightly higher deposition of pCMV-GFP in the pCABOL multilayers than in the pCHIS multilayers.

Since both polymers contain repetitive disulfide linkages in the main chain, the polymers, and therefore the multilayers, can be easily degraded in the presence of the reducing agent DTT, which cleaves the disulfide bonds [51]. In an attempt to get a more direct estimation of pCMV-GFP content, 4 mM DTT was employed to degrade the layers for 1 h and the degradation solution was analyzed on DNA content by PicoGreen assay (Fig. 2B). Interestingly, using this approach the pCABOL multilayers were found to release at least twice as much pCMV-GFP as

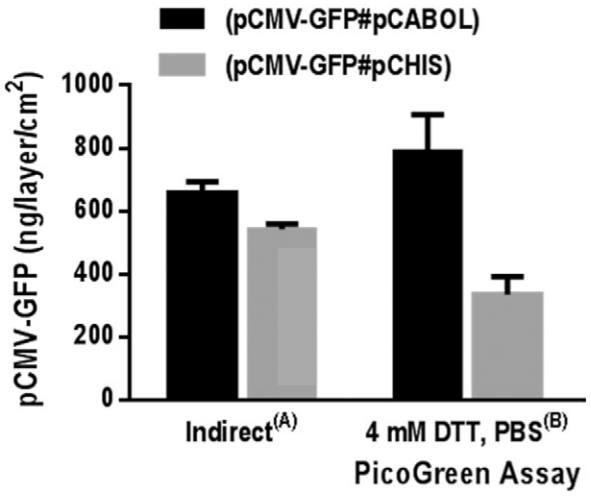

Fig. 2. pCMV-GFP quantification by determination of the remaining concentrations in the deposition solution after multilayer build-up (A), and by PicoGreen assay after multilayer degradation for 1 h in 4 mM DTT in PBS (B).

the pCHIS multilayers. The much lower amount of DNA detected after pCHIS multilayer degradation may be an underestimation due to less release of DNA in this case.

In order to gain further insight about the pCMV-GFP released into cell culture medium, multilayer-coated wells were incubated with cell culture medium for 1 h in the incubator, after which the incubation solutions were loaded into an agarose gel for electrophoresis. Free pCMV-GFP in water and in medium were used as controls. Lanes 1 and 2 of the photograph of the gel under UV illumination (Fig. 3) show that pCABOL and pCHIS multilayers disassemble into plasmid DNA mostly present in its open circular conformation. This finding is in agreement with the report from Zhang et al. [25] which also showed the preferential release of plasmids in the open circular form upon release from the multilayer. The absence of supercoiled pCMV-GFP may indicate the preferred state of pDNA during deposition on the surface. Indeed, an open circular conformation may lead to more multivalent electrostatic binding with the oppositely-charged surface, leading to stronger attachment. The visible bands in the wells of the gel also show the presence of possible polymer-bound pCMV-GFP. This band appears brighter for pCABOL than for pCHIS multilayers. A similar band was not observed for pCMV-GFP dissolved in the cell culture medium (lane 3), indicating that the remaining DNA in the wells is due to binding of pCMV-GFP with PAA polymer and not caused by binding with plasma proteins present in the cell culture medium. For a typical polyplex system, stronger DNA/polymer complexation, for example at higher polymer/DNA ratios, usually leads to less visible bands in the gel wells due to the lower accessibility of the dye to intercalate into the condensed DNA [51]. The differences in fluorescence intensity in the wells in lanes 1 and 2 suggest stronger binding of pCMV-GFP with pCHIS than with pCABOL, in line with the previous discussions. However, a weaker but sufficient interaction between pCABOL and pCMV-GFP for internalization by cells may lead to more efficient unpacking of the pCMV-GFP cargo within the cytoplasm, resulting in better transfection [58].

The results from the PicoGreen assay and the agarose gel electrophoresis may serve as an indication that the difference in transfection capability between the two multilayers is due to the fact that pCABOL multilayers contain and release more pCMV-GFP, and that the pCABOL/pCMV-GFP polyelectrolyte complex is likely more efficient in inducing transfection. It can therefore be concluded that pCABOL-based multilayers are more efficient than pCHIS-multilayers in facilitating surface-mediated cell transfections.

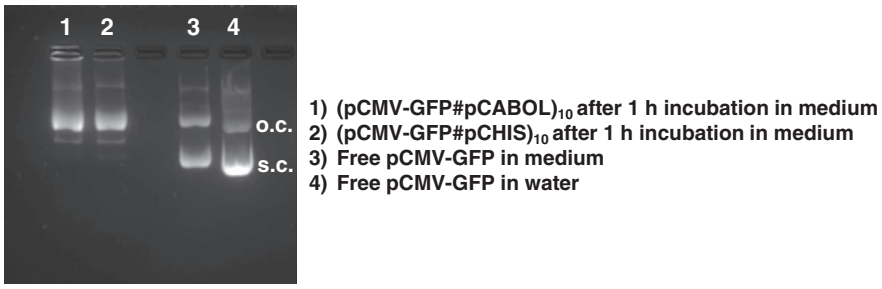

Fig. 3. Agarose gel electrophoresis of cell culture media used to incubate the 10-bilayered pCABOL and pCHIS multilayers (lanes 1 & 2, respectively) and pCMV-GFP solutions in cell culture medium (lane 3) and in water (lane 4) as controls. O.c. = open circular, and s.c. = supercoiled.

3.2. Bilayer Number optimization and metabolic activity

Based on the previous results, the (pCMV-GFP#pCABOL) system was selected for further examination of the number of bilayers necessary for optimal cell transfection, using the intermediate seeding density of 24,000 cells/well. Cells were seeded on multilayers composed of 5, 7, 9.5, 10 and 15 bilayers and the percentage of transfected cells was quantified accordingly (Fig. 4A and B). Cell transfection efficiency increases with increasing bilayer number and reaches a plateau value at 10 to 15 bilayers (Fig. 4B).

Build-up of the pCABOL and pCHIS multilayers proceeds linearly with increasing bilayer numbers [55]. Therefore, it can be expected that a 5-bilayer film would contain and eventually release half of the amount of materials contained in a 10-bilayer film. Fig.4B shows, however, that a 5-bilayer film leads to only ~15% transfection efficiency of that achieved by a 10-bilayer film. Moreover, increasing the bilayer number from 10 to 15 leads only to very small increase in transfection efficiency. Multilayer films composed of only a few bilayers probably supply suboptimal amounts of transfection agent [59], while at bilayer numbers of 10 and higher sufficient transfection agent is released to meet the uptake capacity of the cells growing on the surface, resulting in a plateau value.

Fig. 4B also shows only a minor, although significant ($p < 0.05$), difference in transfection efficiency between 9.5 and 10 bilayers, i.e. multilayers

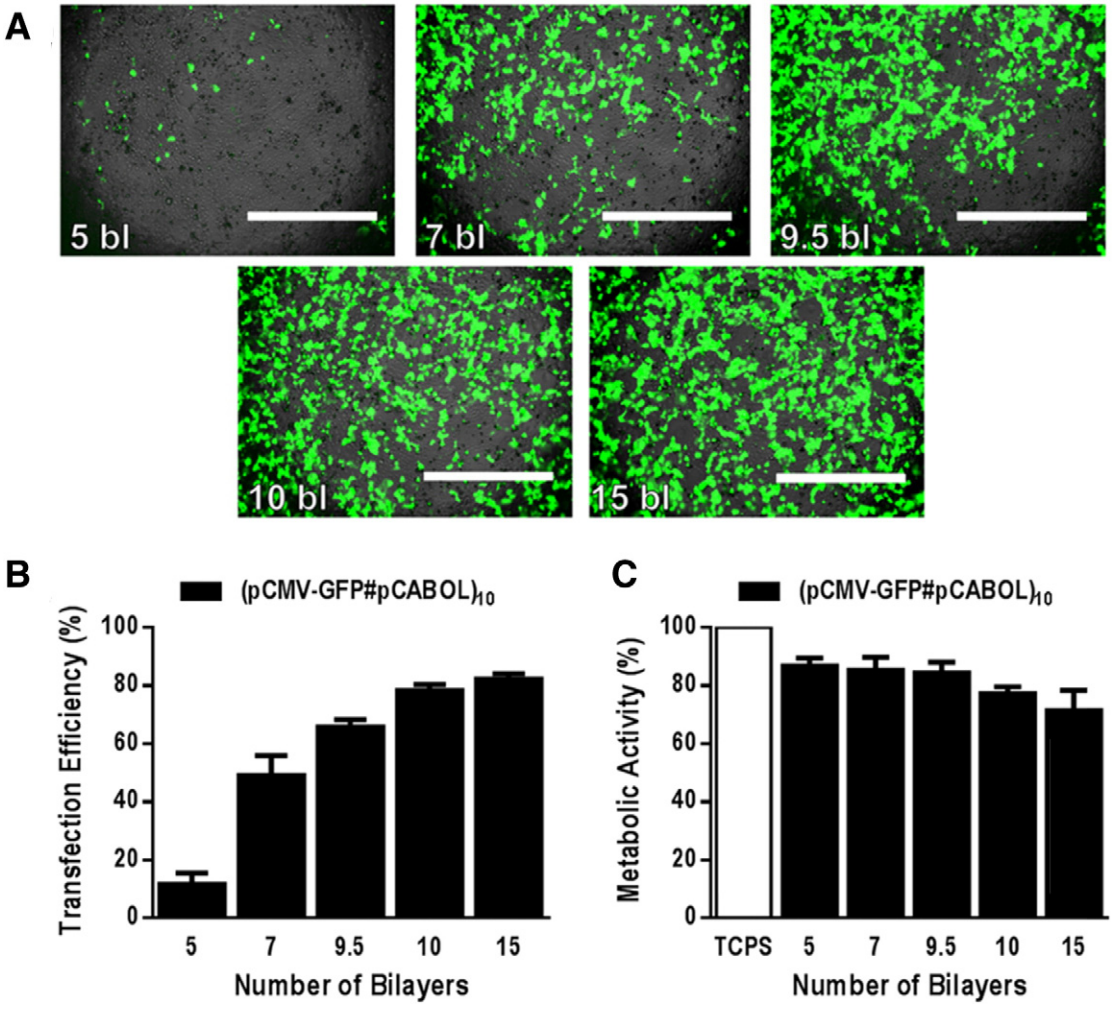

Fig. 4. (A) Overlaid brightfield and GFP images of COS-7 cells 46 h after being cultured on (pCMV-GFP#pCABOL) multilayers with various bilayer numbers at 24,000 cells/well seeding density. Bars = 1000 μm. (B) Transfection efficiency and (C) cell metabolic activity relative to the number of bilayers.

ending with pCMV-GFP and pCABOL layer, respectively. This indicates that the identity of the top layer, either being DNA or pCABOL, only marginally affects cell transfection, which is in agreement with various other reports on alternating DNA-based multilayer coatings [60,61].

Cell metabolic activity in relation to the bilayer number was also analyzed and expressed as a percentage of the metabolic activity of cells seeded on tissue culture plastic (TCPS) (Fig. 4C). Cells seeded on multilayers showed *ca.* 10% lower metabolic activity at lower bilayer numbers, whereas at bilayer numbers 10 and 15 the metabolic activity tends to decrease. However, cells maintained similar shapes throughout the various bilayer numbers studied and are similar to those cultured on TCPS. It has been shown in other studies, that pCABOL and its polyplexes exhibit no or only minor ($\leq$10%) metabolic toxicity to cell cultures [51]. Therefore the further decrease in the metabolic activity at higher bilayer numbers can most probably be attributed to the high GFP production of the cells on these films. It is generally accepted that transfected cells have to spend more efforts towards biosynthesis of the recombinant proteins, leading to a decrease in metabolic activity [56].

3.3. Transfection efficiency of multilayers assembled on various substrates

To test the applicability of the $(pCMV\text{-}GFP\#pCABOL)_{10}$ multilayer to add cell transfecting capability to several common biomaterials, these multilayers were assembled on poly(ε-caprolactone) (PCL), heparinized poly(ε-caprolactone) (PCL-HEP), and poly(lactic acid) (PLA) (Fig. 5A), in a similar way as was previously done with poly-D-lysine (PDL)-coated 96-well plates (PDL-TCPS), but with pCABOL as the precursor layer instead of PDL. The transfection efficiency of COS-7 cells, seeded at a density of 24,000 cells/well and cultured for 48 h on the coated disks is shown in Fig. 5B. The transfection efficiency was found to be slightly higher for PLA disks than for PCL-based disks, and was about similar to the values obtained for PDL–TCPS substrates (Fig. 1B). Despite the increased surface roughness and the presence of a negatively charged surface underneath the multilayer due to the heparin coating, these differences have little effect on the transfection efficiency. The results indicate that the multilayers were formed to a similar extent on the three different substrates and completely mask the properties of the underlying surface at the 10-bilayers utilized. Masking of the underlying substrate was very prominent for PCL and PLA disks, where cell attachment and cell shape were found to be significantly improved after multilayer coating compared to uncoated substrates (data not shown). The reported multilayers therefore not only add cell transfecting capability, but also improve cell adhesion for poor cell-adhering biomaterials.

3.4. 3D plotted scaffold application

To further demonstrate the versatility of the multilayer coating to provide new functionality to various scaffolds and supports for tissue engineering applications, we prepared $(pCMV\text{-}GFP\#pCABOL)_{10}$ multilayers on 3D fiber deposited PCL and PCL-HEP scaffolds. Using this approach, for example, cells can be transfected right at the spot of the implantation site.

3D fiber deposition technique was used for the fabrication of three-dimensional PCL scaffolds, which were subsequently heparinized (for PCL-HEP) and coated with multilayers (Fig. 6). Covalent attachment of heparin already caused a change in the scaffold topography, making the smooth PCL surface topography look rougher. This has been previously reported to facilitate cell adhesion on the material, both because of the increased nano-scaled topography, providing anchor points to cells and also because heparin increases protein adsorption on the surface [54].

Higher magnification SEM images confirmed multilayer coating both on PCL and heparinized PCL, where slight changes can be observed in the scaffold topography with and without multilayer (Fig. 6). The multilayer, approximately 100 nm in thickness [55], conformed to the topography of the original substrates, thus, maintaining the rough feature of heparinized surface, but covering up smaller indentations observed on the surface of the substrates.

When multilayer-covered scaffolds were seeded with COS-7 cells, transfection was observed to occur both on PCL and heparinized PCL scaffolds. The positive transfection observed on the 3D scaffolds were confirmed through the co-localization of GFP-producing cells with the opaque scaffolds. Due to the relatively wide fiber spacing (~600 μm), a significant number of cells fell through the spaces/pores during seeding and subsequently attached and proliferated on the well surface. Some of these cells were also successfully transfected through the transfection agent released into the cell culture medium (data not shown). The availability and use of 3D scaffolds with smaller fiber spacing most likely enable higher seeding densities that can lead to even higher transfection efficiencies.

4. Conclusions

pCABOL and pCHIS, two peptidomimetic linear poly(amido amine)s with differing side groups, have been used to form multilayers with pCMV-GFP as a reporter plasmid. This layer-by-layer strategy was demonstrated to be an effective and inexpensive method to add biofunctionality to biomedical materials of various shapes and sizes. The pCABOL#pCMV-GFP multilayer system proved to be more effective

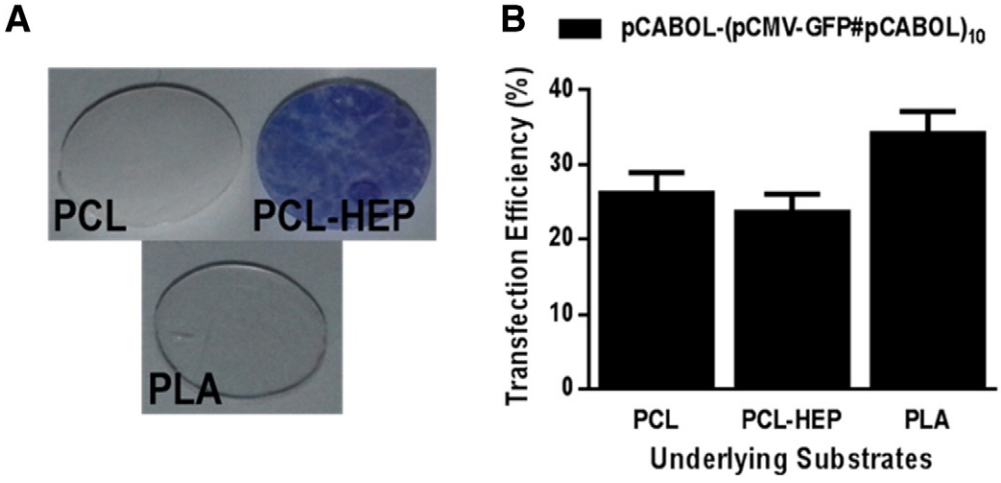

Fig. 5. (A) Digital photograph of the three disks: PCL (white opaque), PCL-HEP (stained with Azure A), and PLA (transparent). (B) Transfection efficiency of COS-7 cells cultured on multilayer-coated disks after 48 h of culture.

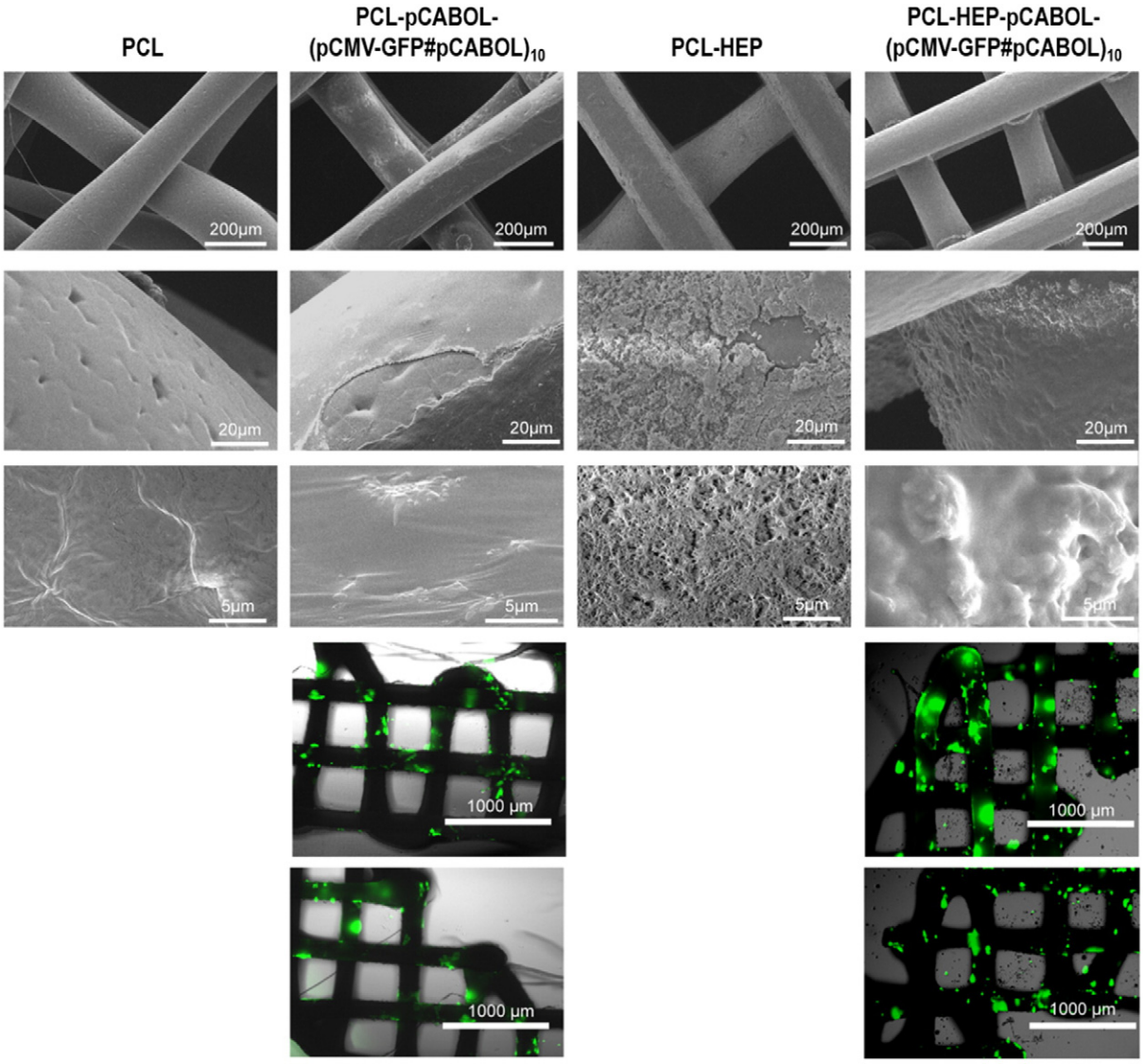

Fig. 6. First three rows: SEM images of 3D fiber PCL and PCL-HEP scaffolds with and without multilayer coating at various magnifications. Two bottom rows: Overlaid brightfield and fluorescence microscopy images of COS-7 cells cultured on the multilayer-coated scaffolds.

in transfection of COS-7 cells cultured on top of these layers than the pHIS#pCMV-GFP system, which is attributed to the higher pCMV-GFP/polymer ratio and higher release of pCMV-GFP in the former system. Transfection efficiency of the pCABOL#pCMV-GFP multilayer system was found to increase with increasing number of bilayers and reached a plateau level at 10–15 bilayers, in which range no significant further increase in transfection efficiency was observed. Cells on top of the multilayers show only small decreases in metabolic activity, which is consistent with the low toxicity of pCABOL and the high production of GFP in the transfected cells.

Various biomedical materials such as PCL, HEP-PCL and PLA were covered with the pCABOL#pCMV-GFP multilayer transfection system and showed significant improvement of cell attachment compared to uncoated substrates. Transfection was found to be equally efficient as when using PDL–TCPS as substrates. Moreover, it was demonstrated that this simple method can also be applied to 3D plotted structures leading to successful transfection of cells adhering on these structures. Such surface-mediated transfection may prove beneficial in various biomedical and tissue engineering applications and provide transfection of cells at the spot of implantation, before and after construct implantation.

Acknowledgments

This work was supported by a grant from the Dutch government to the Netherlands Institute for Regenerative Medicine (NIRM project to S.D.H.). This research was funded by the Diabetes Cell Therapy Initiative (DCTI), the Dutch Diabetes research foundation and the Dutch government through the 2008 FES program (project to G.M.).

References

[1] B.M. Wohl, J.F.J. Engbersen, Responsive layer-by-layer materials for drug delivery, J. Control. Release 158 (2012) 2–14.
[2] Y. Jang, S. Park, K. Char, Functionalization of polymer multilayer thin films for novel biomedical applications, Korean J. Chem. Eng. 28 (2011) 1149–1160.
[3] H. Kerdjoudj, N. Berthelemy, F. Boulmedais, J.F. Stoltz, P. Menu, J.C. Voegel, Multilayered polyelectrolyte films: a tool for arteries and vessel repair, Soft Matter 6 (2010) 3722–3734.
[4] P.T. Hammond, Building biomedical materials layer-by-layer, Mater. Today 15 (2012) 196–206.
[5] J.M. Anderson, A. Rodriguez, D.T. Chang, Foreign body reaction to biomaterials, Semin. Immunol. 20 (2008) 86–100.
[6] Y.X. Sun, K.F. Ren, J.L. Wan, G.X. Chang, J. Ji, Electrochemically controlled stiffness of multilayers for manipulation of cell adhesion, ACS Appl. Mater. Interfaces 5 (2013) 4597–4602.
[7] N. Aggarwal, N. Altgarde, S. Svedhem, G. Michanetzis, Y. Missirlis, T. Groth, Tuning cell adhesion and growth on biomimetic polyelectrolyte multilayers by variation of ph during layer-by-layer assembly, Macromol. Biosci. 13 (2013) 1327–1338.

[8] W.-B. Tsai, Y.-H. Chen, H.-W. Chien, Collaborative cell-resistant properties of polyelectrolyte multilayer films and surface PEGylation on reducing cell adhesion to cytophilic surfaces, J. Biomater. Sci. Polym. Ed. 20 (2009) 1611–1628.
[9] V. Karagkiozaki, E. Vavoulidis, P.G. Karagiannidis, M. Gioti, D.G. Fatouros, I.S. Vizirianakis, S. Logothetidis, Development of a nanoporous and multilayer drug-delivery platform for medical implants, Int. J. Nanomedicine 7 (2012) 5327–5338.
[10] R.C. Smith, M. Riollano, A. Leung, P.T. Hammond, Layer-by-layer platform technology for small-molecule delivery, Angew. Chem. Int. Ed. 48 (2009) 8974–8977.
[11] B. Thierry, P. Kujawa, C. Tkaczyk, F.M. Winnik, L. Bilodeau, M. Tabrizian, Delivery platform for hydrophobic drugs: prodrug approach combined with self-assembled multilayers, J. Am. Chem. Soc. 127 (2005) 1626–1627.
[12] S. Anandhakumar, A.M. Raichur, Polyelectrolyte/silver nanocomposite multilayer films as multifunctional thin film platforms for remote activated protein and drug delivery, Acta Biomater. 9 (2013) 8864–8874.
[13] X. Su, B.-S. Kim, S.R. Kim, P.T. Hammond, D.J. Irvine, Layer-by-layer-assembled multilayer films for transcutaneous drug and vaccine delivery, ACS Nano 3 (2009) 3719–3729.
[14] M. Keeney, M. Mathur, E. Cheng, X. Tong, F. Yang, Effects of polymer end-group chemistry and order of deposition on controlled protein delivery from layer-by-layer assembly, Biomacromolecules 14 (2013) 794–800.
[15] M.L. Macdonald, R.E. Samuel, N.J. Shah, R.F. Padera, Y.M. Beben, P.T. Hammond, Tissue integration of growth factor-eluting layer-by-layer polyelectrolyte multilayer coated implants, Biomaterials 32 (2011) 1446–1453.
[16] I.C. Lee, Y.-C. Wu, Facilitating neural stem/progenitor cell niche calibration for neural lineage differentiation by polyelectrolyte multilayer films, Colloids Surf. B: Biointerfaces 121 (2014) 54–65.
[17] P.-W. Fu, S.-Y. Wang, Y.-R. Chen, C.-M. Lo, Cardiomyocyte differentiation of mouse iPSCs regulated by polypeptide multilayer films (1180.21), FASEB J. 28 (2014).
[18] J. Hong, L. Alvarez, N. Shah, Y. Cho, B.-S. Kim, L. Griffith, K. Char, P. Hammond, Multilayer thin-film coatings capable of extended programmable drug release: application to human mesenchymal stem cell differentiation, Drug Deliv. Transl. Res. 2 (2012) 375–383.
[19] K.F. Ren, T. Crouzier, C. Roy, C. Picart, Polyelectrolyte multilayer films of controlled stiffness modulate myoblast cell differentiation, Adv. Funct. Mater. 18 (2008) 1378–1389.
[20] J. Blacklock, Y.Z. You, Q.H. Zhou, G. Mao, D. Oupicky, Gene delivery in vitro and in vivo from bioreducible multilayered polyelectrolyte films of plasmid DNA, Biomaterials 30 (2009) 939–950.
[21] D. Richard, I. Nguyen, C. Affolter, F. Meyer, P. Schaaf, J.C. Voegel, D. Bagnard, J. Ogier, Polyelectrolyte multilayer-mediated gene delivery for semaphorin signaling pathway control, Small 6 (2010) 2405–2411.
[22] E.M. Saurer, R.M. Flessner, S.P. Sullivan, M.R. Prausnitz, D.M. Lynn, Layer-by-layer assembly of DNA- and protein-containing films on microneedles for drug delivery to the skin, Biomacromolecules 11 (2010) 3136–3143.
[23] C.M. Jewell, D.M. Lynn, Multilayered polyelectrolyte assemblies as platforms for the delivery of DNA and other nucleic acid-based therapeutics, Adv. Drug Deliv. Rev. 60 (2008) 979–999.
[24] Y. Lvov, G. Decher, G. Sukhorukov, Assembly of thin films by means of successive deposition of alternate layers of DNA and poly(allylamine), Macromolecules 26 (1993) 5396–5399.
[25] J.T. Zhang, L.S. Chua, D.M. Lynn, Multilayered thin films that sustain the release of functional DNA under physiological conditions, Langmuir 20 (2004) 8015–8021.
[26] C.M. Jewell, J. Zhang, N.J. Fredin, M.R. Wolff, T.A. Hacker, D.M. Lynn, Release of plasmid DNA from intravascular stents coated with ultrathin multilayered polyelectrolyte films, Biomacromolecules 7 (2006) 2483–2491.
[27] E.M. Saurer, C.M. Jewell, D.A. Roenneburg, S.L. Bechler, J.R. Torrealba, T.A. Hacker, D.M. Lynn, Polyelectrolyte multilayers promote stent-mediated delivery of DNA to vascular tissue, Biomacromolecules 14 (2013) 1696–1704.
[28] P.C. DeMuth, X. Su, R.E. Samuel, P.T. Hammond, D.J. Irvine, Nano-layered microneedles for transcutaneous delivery of polymer nanoparticles and plasmid DNA, Adv. Mater. 22 (2010) 4851–4856.
[29] F. Meyer, V. Ball, P. Schaaf, J.C. Voegel, J. Ogier, Polyplex-embedding in polyelectrolyte multilayers for gene delivery, Biochim. Biophys. Acta Biomembr. 1758 (2006) 419–422.
[30] J.K. Sun, K.F. Ren, L.Z. Zhu, J. Ji, Multilayers based on cationic nanocomplexes for co-delivery of doxorubicin and DNA, Colloids Surf. B 112 (2013) 67–73.
[31] Y. Hu, K. Cai, Z. Luo, C. Chen, H. Dong, J. Hao, L. Yang, L. Deng, Fabrication of galactosylated polyethylenimine and plasmid DNA multilayers on poly (D, L-lactic acid) films for in situ targeted gene transfection, Adv. Eng. Mater. 11 (2009) B30–B34.
[32] N.W. Kim, M.S. Lee, K.R. Kim, J.E. Lee, K. Lee, J.S. Park, Y. Matsumoto, D.G. Jo, H. Lee, D.S. Lee, J.H. Jeong, Polyplex-releasing microneedles for enhanced cutaneous delivery of DNA vaccine, J. Control. Release 179 (2014) 11–17.
[33] P.C. DeMuth, A.V. Li, P. Abbink, J. Liu, H. Li, K.A. Stanley, K.M. Smith, C.L. Lavine, M.S. Seaman, J.A. Kramer, A.D. Miller, W. Abraham, H. Suh, J. Elkhader, P.T. Hammond, D.H. Barouch, D.J. Irvine, Vaccine delivery with microneedle skin patches in nonhuman primates, Nat. Biotechnol. 31 (2013) 1082–1085.
[34] X. Guo, Q.X. Zheng, I. Kulbatski, Q. Yuan, S.H. Yang, Z.W. Shao, H. Wang, B.J. Xiao, Z.Q. Pan, S. Tang, Bone regeneration with active angiogenesis by basic fibroblast growth factor gene transfected mesenchymal stem cells seeded on porous beta-TCP ceramic scaffolds, Biomed. Mater. 1 (2006) 93–99.
[35] B.A. Borden, J. Yockman, S.W. Kim, Thermoresponsive hydrogel as a delivery scaffold for transfected rat mesenchymal stem cells, Mol. Pharm. 7 (2010) 963–968.
[36] W.W. Thein-Han, J. Saikhun, C. Pholpramoo, R.D.K. Misra, Y. Kitiyanant, Chitosan–gelatin scaffolds for tissue engineering: physico-chemical properties and biological response of buffalo embryonic stem cells and transfectant of GFP-buffalo embryonic stem cells, Acta Biomater. 5 (2009) 3453–3466.
[37] Y.B. Xie, S.T. Yang, D.A. Kniss, Three-dimensional cell-scaffold constructs promote efficient gene transfection: implications for cell-based gene therapy, Tissue Eng. 7 (2001) 585–598.
[38] C. Sapet, C. Formosa, F. Sicard, E. Bertosio, O. Zelphati, N. Laurent, 3D-fection: cell transfection within 3D scaffolds and hydrogels, Ther. Deliv. 4 (2013) 673–685.
[39] J.H. Jang, C.B. Rives, L.D. Shea, Plasmid delivery in vivo from porous tissue-engineering scaffolds: transgene expression and cellular Transfection, Mol. Ther. 12 (2005) 475–483.
[40] Y. Yang, X. Li, L. Cheng, S. He, J. Zou, F. Chen, Z. Zhang, Core–sheath structured fibers with pDNA polyplex loadings for the optimal release profile and transfection efficiency as potential tissue engineering scaffolds, Acta Biomater. 7 (2011) 2533–2543.
[41] X. Zhao, D. Komatsu, M. Hadjiargyrou, BMP-2 delivery using Electrospun PLLA/collagen I scaffolds with surface adsorbed plasmid DNA/transfection complexes, J. Bone Miner. Res. 28 (2013) 2.
[42] Y. Kido, J.-i. Jo, Y. Tabata, A gene transfection for rat mesenchymal stromal cells in biodegradable gelatin scaffolds containing cationized polysaccharides, Biomaterials 32 (2011) 919–925.
[43] H.D. Lu, L.L. Lv, Y.H. Dai, G. Wu, H.Q. Zhao, F.C. Zhang, Porous chitosan scaffolds with embedded hyaluronic acid/chitosan/plasmid-DNA nanoparticles encoding TGF-beta 1 induce DNA controlled release, transfected chondrocytes, and promoted cell proliferation, PLoS One 8 (2013) 13.
[44] M. Keeney, J. van den Beucken, P.M. van der Kraan, J.A. Jansen, A. Pandit, The ability of a collagen/calcium phosphate scaffold to act as its own vector for gene delivery and to promote bone formation via transfection with VEGF(165), Biomaterials 31 (2010) 2893–2902.
[45] X. Yu, W.L. Murphy, 3-D scaffold platform for optimized non-viral transfection of multipotent stem cells, J. Mater. Chem. B 2 (2014) 8186–8193.
[46] N. Jessel, M. Oulad-Abdelghani, F. Meyer, P. Lavalle, Y. Haîkel, P. Schaaf, J.-C. Voegel, Multiple and time-scheduled in situ DNA delivery mediated by β-cyclodextrin embedded in a polyelectrolyte multilayer, Proc. Natl. Acad. Sci. U. S. A. 103 (2006) 8618–8621.
[47] C. Holmes, J. Daoud, P.O. Bagnaninchi, M. Tabrizian, Polyelectrolyte multilayer coating of 3D scaffolds enhances tissue growth and gene delivery: non-invasive and label-free assessment, Adv. Healthc. Mater. 3 (2014) 572–580.
[48] P. Vader, L. van der Aa, J.J. Engbersen, G. Storm, R. Schiffelers, Physicochemical and biological evaluation of siRNA polyplexes based on PEGylated poly(amido amine)s, Pharm. Res. 29 (2012) 352–361.
[49] G. Coué, C. Freese, R.E. Unger, C. James Kirkpatrick, J.F.J. Engbersen, Bioresponsive poly(amidoamine)s designed for intracellular protein delivery, Acta Biomater. 9 (2013) 6062–6074.
[50] M. Piest, J.F.J. Engbersen, Effects of charge density and hydrophobicity of poly(amido amine)s for non-viral gene delivery, J. Control. Release 148 (2010) 83–90.
[51] C. Lin, Z. Zhong, M.C. Lok, X. Jiang, W.E. Hennink, J. Feijen, J.F.J. Engbersen, Novel bioreducible poly(amido amine)s for highly efficient gene delivery, Bioconjug. Chem. 18 (2006) 138–145.
[52] A. Zintchenko, L.J. van der Aa, J.F. Engbersen, Improved synthesis strategy of poly(amidoamine)s for biomedical applications: catalysis by “green” biocompatible earth alkaline metal salts, Macromol. Rapid Commun. 32 (2011) 321–325.
[53] S. Singh, B.M. Wu, J.C.Y. Dunn, Accelerating vascularization in polycaprolactone scaffolds by endothelial progenitor cells, Tissue Eng. A 17 (2011) 1819–1830.
[54] S. Singh, B.M. Wu, J.C.Y. Dunn, The enhancement of VEGF-mediated angiogenesis by polycaprolactone scaffolds with surface cross-linked heparin, Biomaterials 32 (2011) 2059–2069.
[55] S.D. Hujaya, J.M.J. Paulusse, J.F.J. Engbersen, Multilayered thin films from poly(amido amine)s and DNA, Acta Biomater. (2015) (accepted for publication).
[56] C.Y.M. Hsu, H. Uludag, A simple and rapid nonviral approach to efficiently transfect primary tissue-derived cells using polyethylenimine, Nat. Protoc. 7 (2012) 935–945.
[57] J.J.J.P. van den Beucken, M.R.J. Vos, P.C. Thüne, T. Hayakawa, T. Fukushima, Y. Okahata, X.F. Walboomers, N.A.J.M. Sommerdijk, R.J.M. Nolte, J.A. Jansen, Fabrication, characterization, and biological assessment of multilayered DNA-coatings for biomaterial purposes, Biomaterials 27 (2006) 691–701.
[58] D.V. Schaffer, N.A. Fidelman, N. Dan, D.A. Lauffenburger, Vector unpacking as a potential barrier for receptor-mediated polyplex gene delivery, Biotechnol. Bioeng. 67 (2000) 598–606.
[59] S.S. Ono, G. Decher, Preparation of ultrathin self-standing polyelectrolyte multilayer membranes at physiological conditions using pH-responsive film segments as sacrificial layers, Nano Lett. 6 (2006) 592–598.
[60] J.J. van den Beucken, X.F. Walboomers, M.R. Vos, N.A. Sommerdijk, R.J. Nolte, J.A. Jansen, Biological responses to multilayered DNA-coatings, J. Biomed. Mater. Res. B Appl. Biomater. 81 (2007) 231–238.
[61] T. Fukushima, Y. Inoue, T. Hayakawa, K. Taniguchi, K. Miyazaki, Y. Okahata, Preparation of and tissue response to DNA–lipid films, J. Dent. Res. 80 (2001) 1772–1776.